Audio Engineering Society
Convention Paper
Presented at the 114th Convention
2003 March 22–25 Amsterdam, The Netherlands

Analysis of a Folded Horn

Andrew Bright [1] [2]

[1] Nokia Group, FIN-00045, Helsinki, Finland

[2] Section of Acoustic Technology, Ørsted·DTU, Technical University of Denmark, Lyngby, Denmark

ABSTRACT

A boundary element model is used to analyse a folded horn. Results from the boundary element model are compared to measurements of the throat radiation impedance and the far-field acoustic response. Further analysis shows how one-dimensional and lumped parameter models can be derived from the boundary element results, and used to gain insight into the behaviour of the folded horn loudspeaker system. It is shown that one type of folded horn behaves more like a vented-box than a traditional horn-loaded loudspeaker system.

1. Introduction

The addition of a horn to a loudspeaker can greatly increase its efficiency. The horn acts as a mechano-acoustic transfer, increasing the effective impedance presented by air to a loudspeaker driver's diaphragm.

Traditional horns can be analysed with analytical or simple numerical tools. Using these tools to analyse a folded horn, however, is complicated by the fact that the flare rate of the folded horn is not readily evident. For this reason, the boundary element method (BEM) has been used to analyse a simple folded horn in this paper.

The BEM model has been used to calculate the radiation impedance and transfer impedance of the horn. In combination with a lumped-parameter model of the loudspeaker driver, these results are used to simulate the acoustic pressure-to-voltage response of a complete folded-horn loudspeaker. All simulation results are compared to measurement

Analyses of BEM and measurement results give insight into the one-parameter behaviour of the folded horn under study. It is found that lumped-parameter models can capture dominant features of the horn's radiation impedance and transfer impedance. Analysis of this lumped parameter model shows that the folded horn under study affects the loudspeaker's response more like that of a bass-reflex enclosure than a traditional infinite-length horn.

1.1. Simulation – general method

The effect on the acoustic response of adding a horn to a loudspeaker is analysed in this paper by the following general method. The loudspeaker's

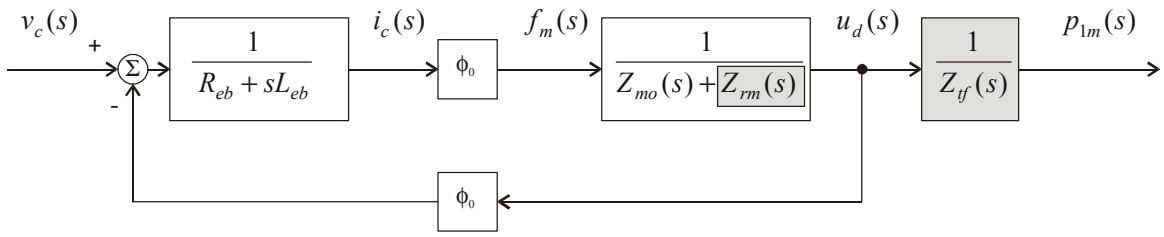

Figure 1: Block diagram of dynamic system representation of the standard lumped-parameter model of the electrodynamic loudspeaker.

diaphragm is assumed to be rigid, i.e. it vibrates as a single lumped mass, with no higher-order modal behaviour. This is the standard single-degree-of freedom model of the electrodynamic loudspeaker, as discussed by classical texts on loudspeakers. This model may be presented as the dynamic system shown in Figure 1, after the form presented by Knudsen et al. [1].

This model may be used to simulate the ratio of acoustic pressure $p_{1m}(s)$ to input voltage $v_c(s)$. Within the context of this model, the addition of a horn to the loudspeaker affects the mechanical-equivalent acoustic radiation impedance, or horn-loading impedance $Z_{rm}(s)$, and the acoustic transfer impedance $Z_{tf}(s)$, highlighted in grey in Figure 1. This framework is generally similar to a method presented by Geddes and Clark [2]. Prediction of the effect of the acoustic horn, therefore, requires calculation of these two transfer functions. With these two transfer functions, the ratio of acoustic pressure to input voltage may be calculated from:

$$\frac{p_r(s)}{v_c(s)} = \frac{\phi_0}{Z_{eb}(s)\left(Z_{mo}(s)+Z_{rm}(s)\right)+\phi_0^2} Z_{tf}(s) \quad (1)$$

where the terms in (1) are as follows:

- $p_r(s)$ acoustic pressure at a distance r from the loudspeaker
- $v_c(s)$ voltage-drop across the ends of the voice-coil
- $Z_{eb}(s)$ blocked electrical impedance; electrical input impedance of the loudspeaker under mechanically fixed conditions
- $Z_{mo}(s)$ open-circuit mechanical impedance, including the effects of the rear-acoustic mounting of the loudspeaker.
- $Z_{rm}(s)$ mechanical-equivalent acoustic radiation impedance presented by the horn to the loudspeaker
- $Z_{tf}(s)$ transfer impedance; ratio of diaphragm velocity to acoustic pressure $p_r(s)$
- ϕ_0 transduction coefficient (B·l product, or force factor)

A wide range of methods may be used to calculate the horn-loading impedance and transfer impedance transfer functions. The oldest method relies on an analytical solution to this one-dimensional wave equation with varying cross-sectional area:

$$\frac{\partial^2}{\partial t^2} p(x,t) = c_0^2 \frac{1}{S(x)} \frac{\partial}{\partial x}\left(S(x) \frac{\partial}{\partial x} p(x,t) \right) \quad (2)$$

where the terms in (2) are as follows:

- $p(x,t)$ acoustic pressure
- x distance along axis of symmetry of horn
- t time
- $S(x)$ flare rate, i.e. the cross-sectional area of horn as function of distance along axis of symmetry, x, as shown in Figure 2;
- c_0 speed of sound

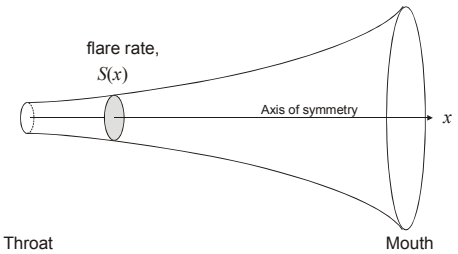

Figure 2: Definition of the flare rate, $S(x)$, for a horn.

Equation (2) is commonly known among acousticians as 'Webster's horn equation,' due to Webster's 1919 publication describing how it can be used to analyse phonograph horns [3]. Hanna and Slepian later applied the same theory in 1924 [4] to horn-loaded loudspeakers, though these latter authors make no reference to Webster. This parallel 'discovery' of the usability of (2) for engineering analysis of the acoustic horn is somewhat explained by Edward Eisner's 1964 discussion [5] on the history of (2), wherein Eisner notes it was first developed and solved for an acoustic horn in a paper published in 1764 by Daniel Bernoulli [6]. All this history aside, the reader interested in more detail on the development of (2) is referred to readily available basic textbooks on loudspeakers, e.g. Olson [7] or Beranek [8], among others.

The primary limitation, from the point of view of a loudspeaker designer, to using analytical solutions to (2) for analysing horns is that such solutions are available for a limited number of horn flare rates. Specifically, as noted by Holland et al. [9], it can be solved only for cylindrical, conical, exponential, and hyperbolic flare rates, plus flare rates described as combinations between exponential hyperbolic rates (this being described by Salmon [10]).

It was shown by Holland et al. [9] that a horn of arbitrary flare rate can be analysed by subdividing the horn into small sections of flare rate for which an analytical solution to (2) is available. For example, one may 'fit' some arbitrary flare rate with short sections of cylindrical, conical, or exponential curves. The input and transfer of impedances of each of these sections can be determined analytically from solutions to (2). These may be collected together as a sectioned transmission line model of varying impedance, from which the total input and transfer impedance may be calculated. Thus, with the aid of a computer with computational power not much more than that of a retractable pen, the complete electro-acoustic response of a loudspeaker loaded with such a horn may be calculated in the context of Figure 1.

1.2. Single parameter models

Morse (1953) [11] explains that (2) is more generally applicable if the horn under investigation admits to a one-parameter (1P) wave, i.e. all the acoustic quantities can be defined by a single spatial coordinate. Although Morse admits the existence of exact one-parameter solutions to (2) for very few coordinate systems, he used the 1P assumption to develop approximate solutions to more complex shapes. Putland (1993) [12] seems to be the first author to actually specify the only three coordinate systems that produce *exact* solutions for one parameter wavefields: planar (1-D), cylindrical (2-D), and spherical (3-D). Putland notes that these and only these coordinate systems are capable of exactly specifying all the acoustic quantities (pressure, particle velocity, intensity, etc.) by a single spatial coordinate. Lack of this strict degree of mathematical exactness does not, however, seem to have prevented effective one-parameter analysis on a variety of more complicated horn geometries.

It is explained by Holland et al. [9] that the effective cross-sectional area of a wave propagating through a horn will tend to be larger than would be predicted assuming plane-wave propagation. Although the wave may exhibit one-parameter behaviour, and thus will be a solution to (2), the flare rate function $S(x)$ will not follow the planar cross-sectional area of the horn. The work of Holland et al. [9] suggests that actual wavefronts will be somewhere between planar and spherical in shape, suggesting a slight increase in the flare rate function $S(x)$ over the planar flare rate, though no quantitative data is provided.

1.3. Folded horns

The lower limit of the range of usable frequencies of a horn is determined by the ratio of its length to flare rate. For proper operation at low frequencies (down to some 50Hz), this requires horns of some five (5) metres in length. Horns of such long length are impractical for the majority of loudspeaker applications. Designers have circumvented this problem by 'folding' or bending the horn at one or more points along its length. Perhaps the most famous (if not the first) such 'folded horn' was the 'Klipschorn' described by Klipsch in 1944 [13]. This type of 'folded horn' for low-frequency loudspeakers enjoyed some commercial success for domestic use. More recently, other types of folded horns have become common in loudspeaker systems for sound reinforcement and large-scale public address.

In the design process of a folded horn, using Equation (2) is complicated by one fact: It is considerably less obvious what the flare rate function $S(x)$ should be from the horn's geometry than for more traditional horns. Consider the sectional view of the simple folded horn shown in Figure 3. In contrast to the axisymmetric horn shown in Figure 2, it is at first not obvious where the effective axis of symmetry should be drawn, nor then clear what the effective area of the wavefront propagating through

the horn along such an axis would be. A boundary element method simulation was performed to gain insight into this type of horn's one-parameter behaviour.

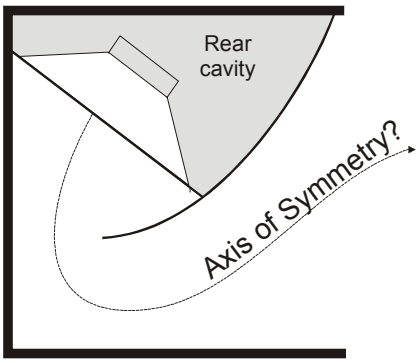

Figure 3: Sectional view of a simple folded horn.

1.4. Boundary Element Method

The boundary element method (BEM) can be used to analyse the acoustic radiation characteristics of any arbitrarily shaped object. Also known as the Integral-equation method, it uses a discretisation of the surface of an object and a set of velocity or pressure boundary conditions to calculate an acoustic field, either into a free-field, or into an enclosed space. Brebbia (1991) [14] provides a well-known but somewhat out-of-date[a] review of boundary element theory for acoustics. Wu (2001) [15] provides a more up-to-date review of BEM theory.

There are two basic formulations of the BEM method:

- Direct (collocational) method
- Indirect variational method

These two methods have a somewhat different theoretical formulation. Functionally, the indirect method can simulate very thin structures without large element size, although it can have larger memory requirements and longer computational times than the direct method. Due to the thin exterior walls of the folded horn under analysis in this paper, it was found that the indirect variational method was by far the more efficient of these two methods for this structure.

All BEM computation reported in this paper was done using the commercial software package SYSNOISE, version 5.0.

1.5. BEM simulations of a folded horn

The mesh describing the folded horn under study used in the BEM model is shown in Figure 4 and Figure 5. In Figure 5, elements on the top and side of the exterior surface of the mesh have been removed, to show the interior detail of the mesh.

The mesh consists of about 1000 nodes and elements. Linear elements were used, i.e. one node per element edge. Computation time was approximately 1 hour per frequency, using an Intel 486 66MHz based PC.[b]

For scale, the overall size of the horn shown in Figure 4 and Figure 5 is approximately 0.45 × 0.75 × 0.75 m.

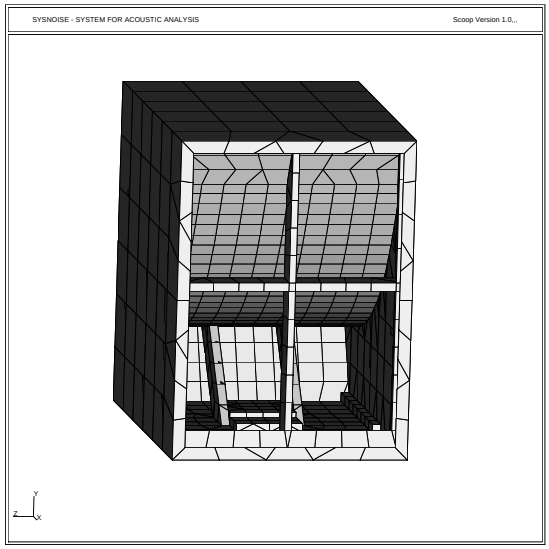

Figure 4: Complete mesh, exterior view.

[a] …as well as out-of-print…

[b] The simulation was performed in mid-1995.

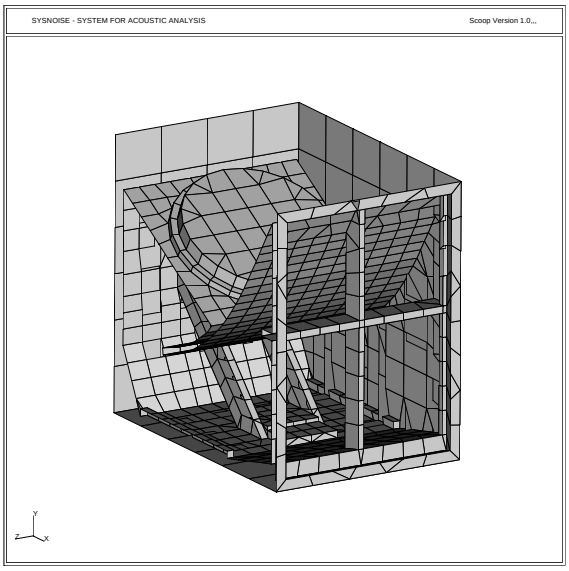

Figure 5: View from corner, with top & side elements removed, to show interior of mesh.

As described above, the BEM model has been used to compute two aspects of the horn:

- Acoustic radiation impedance
- Transfer impedance

In the boundary element model, those elements that are located where the loudspeaker diaphragm would be have been set to have a boundary condition of unity (1) surface-normal velocity. With this boundary condition (assuming a rigid diaphragm), the acoustic radiation impedance can by BEM computation by taking the mean value of the acoustic pressure at the nodes of these diaphragm elements, scaled by the effective area of the diaphragm. The transfer impedance, defined as the ratio of acoustic pressure at a field point of interest to the diaphragm velocity, is simply the acoustic pressure calculated by the BEM model at this field point.

To further ensure correct calculation of the BEM results, a small modification was made to the BEM mesh. A 120mm extension to the 'tongue' of the folded horn, as per Figure 6, was added in both the mesh used for BEM analysis and in the experimental unit under test.

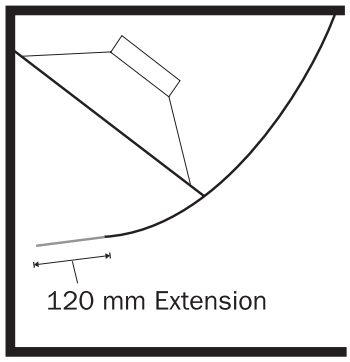

Figure 6: Extension of the 'tongue' of the folded horn. This modification was made in a BEM mesh as well as in an experimental unit.

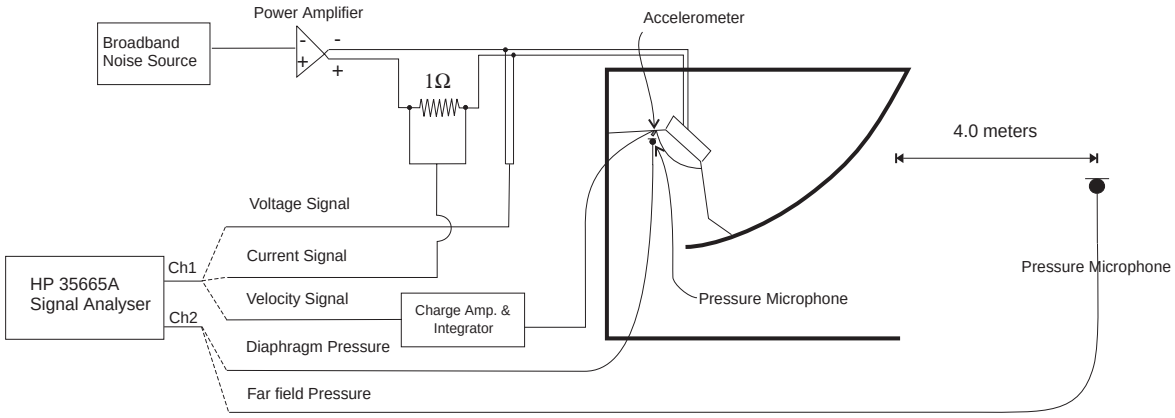

Figure 7: Block diagram of experimental set-up for measurement of radiation impedance and transfer impedance. The loudspeaker was placed in an anechoic room for the measurement.

1.6. Verification of BEM results

The radiation and transfer impedance were measured directly, in order to verify the results of the BEM model.

A block diagram of the experimental set-up for measuring the radiation impedance and transfer impedance is shown in Figure 7.

A comparison of the real and imaginary parts of the radiation impedance between that predicted by the BEM model and that measured is shown in Figure 8. The dB magnitude of the same is shown in Figure 9. As can be seen in these figures, the measured impedance closely matches the results from the BEM model.

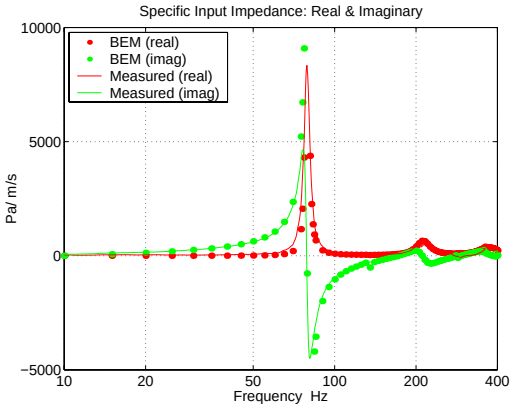

Figure 8: Radiation impedance (real & imaginary), from BEM model and measurement.

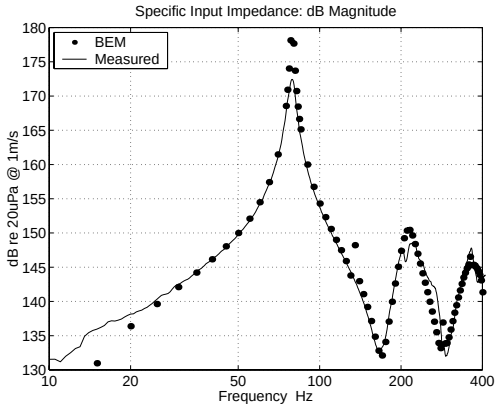

Figure 9: Radiation impedance (dB magnitude), from BEM model and measurement.

A comparison of the transfer impedance between results from the BEM model and the direct measurement is shown in Figure 10. The agreement between the two is generally good, except at frequencies below 50Hz and between 200 Hz – 300 Hz. It is expected that the discrepancy below 50 Hz is due to the inability of the anechoic room in which the measurement was made to properly re-create free-field conditions at these low frequencies. (The nominal cut-off frequency of the room concerned is 70Hz) The discrepancy between 200 Hz – 300 Hz is due to non-rigid behaviour of the diaphragm, causing a single-point vibration measurement to give a poor estimate of the volume velocity of the loudspeaker.

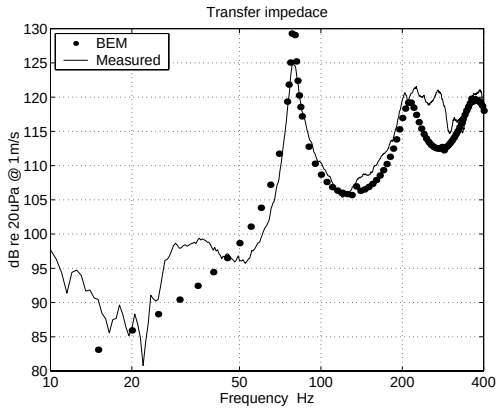

Figure 10: Transfer impedance (dB magnitude), from BEM model and measurement.

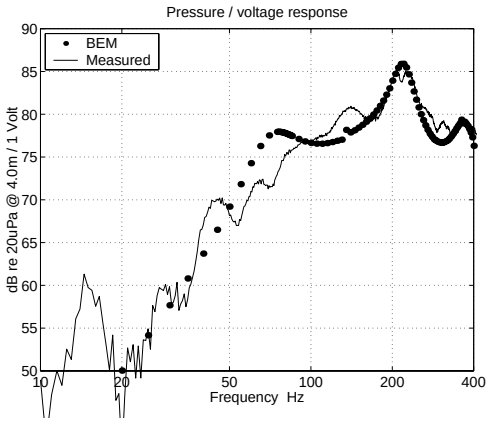

Figure 11: Pressure (on-axis, far-field), to voltage ratio (dB), using BEM results in (1), vs. direct measurement.

Results for the modified horn (as per Figure 6), are shown in Figure 12 (dB magnitude of impedance) and Figure 13 (pressure to voltage ratio). These figures show that the BEM calculation is able to correctly predict the change in the acoustic behaviour caused by the 'tongue' extension shown in Figure 6.

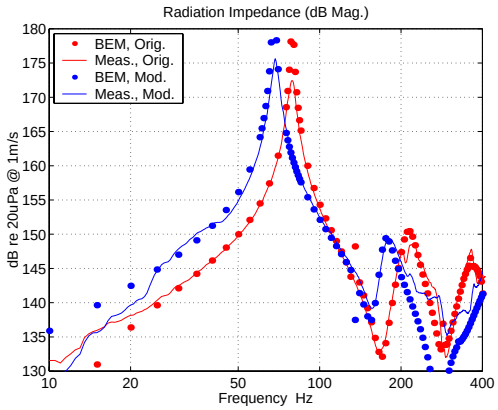

Figure 12: Radiation impedance: original vs. modified horn (as per Figure 6), measured & BEM results.

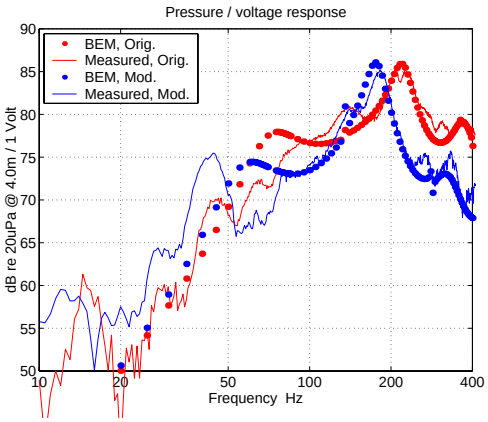

Figure 13: Pressure (on-axis, far-field) to voltage ratio (dB): original vs. modified horn (as per Figure 6).

2. One-parameter behaviour of the folded horn

The one-parameter behaviour of the folded-horn under study is analysed by plotting the contour lines of constant phase on a post-processing grid within the horn. These are shown in Figure 14 – Figure 18.

As can be seen in these figures, the one-parameter behaviour of the horn seems to be approximately hyperbolic, i.e. at first a constriction, followed by a length of roughly constant cross-section, and then the area of expansion.

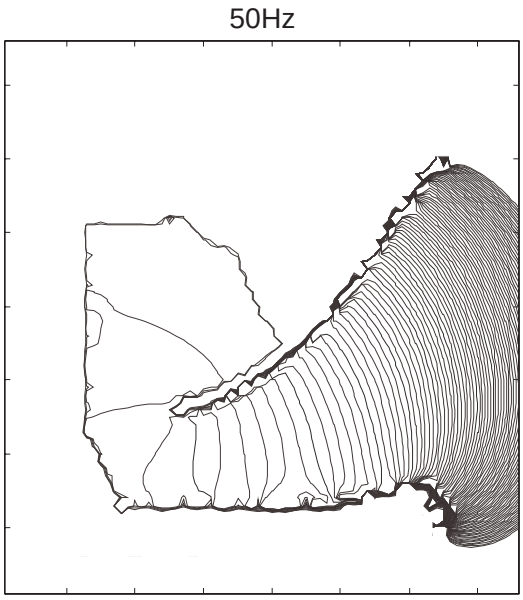

Figure 14: Isophase contours at 50Hz.

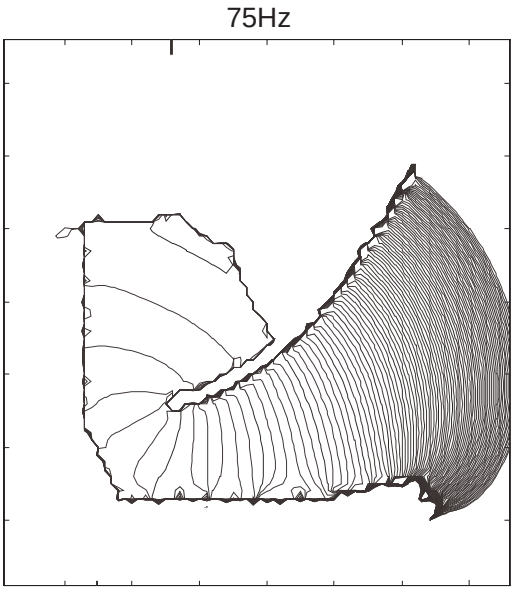

Figure 15: Isophase contours at 75Hz.

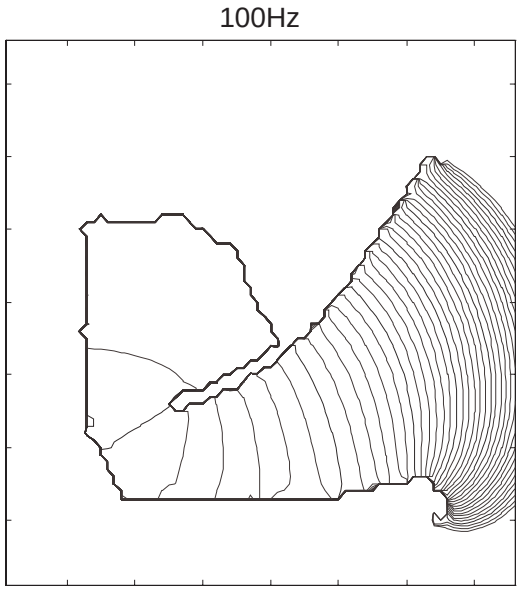

Figure 16: Isophase contours at 100Hz.

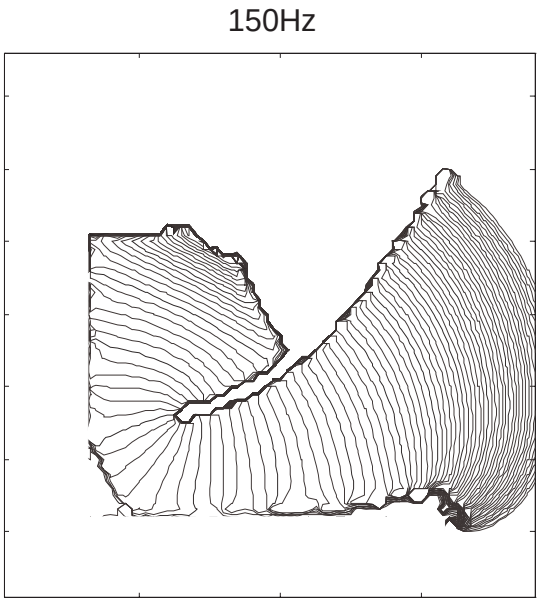

Figure 17: Isophase contours at 150Hz.

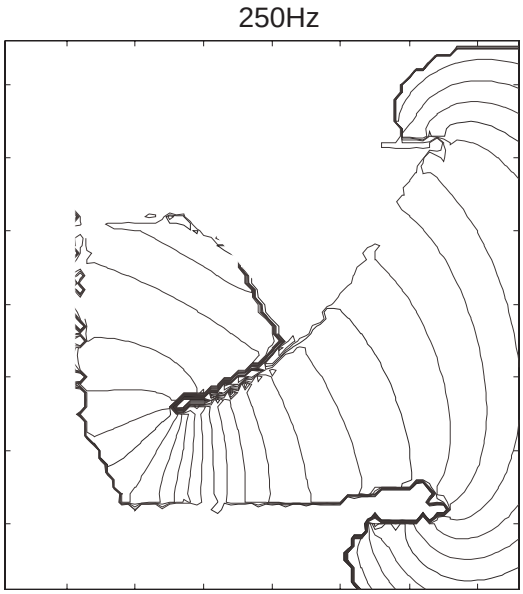

Figure 18: Isophase contours at 250Hz.

3. Synthesis

As per Figure 8 through Figure 10, the dominant feature of the radiation and transfer impedance is the large resonance occurring at 78Hz. It is thus considered that the basic properties of the horn could be specified for a given driver in much the same way as a bass-reflex cabinet can be done, after the method published by Thiele (1961) [16]. This specification process, taking terminology from active analogue filter design, is generally referred to as synthesis.

The process of synthesis assumes lumped-parameter approximations to the radiation and transfer impedance. It is assumed that the radiation impedance can be modelled by a single-degree-of-freedom (SDOF) system as so:

$$\hat{Z}_{rm}(s) = \frac{1}{m_{rm}} \frac{s}{\left(s - \lambda_{rm}\right)\left(s - \lambda_{rm}^{*}\right)} \qquad (3)$$

The accuracy of this model by comparison to the BEM simulations results is shown in Figure 19. As can be seen in this figure, the SDOF model captures the main resonance, but not the higher resonances occurring at 210 Hz and 360 Hz.

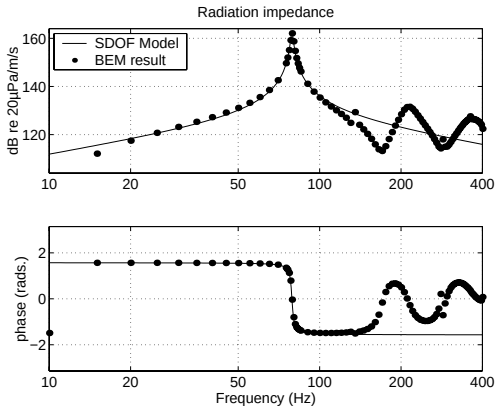

Figure 19: SDOF model of the radiation impedance.

The transfer impedance can be modelled by a similar, by first separating between the monopole radiation aspects and that contributed by the horn, as so:

$$\hat{Z}_{tf}(s) = \rho_0 S_d \; s \; \frac{e^{ikr}}{4\pi r} \; Z_{tf \cdot h}(s) \qquad (4)$$

where the terms in (4) are as follows:

$Z_{tf \cdot h}(s)$	horn-induced non-monopole radiation characteristics
ρ_0	density of air
S_d	effective area of the loudspeaker
s	Laplace variable, = $i2\pi f$

In (4), $Z_{tf \cdot h}(s)$ describes the effects on the radiation caused by the horn, and all other terms on the RHS are associated with free-field acoustic radiation from a monopole source. In this way, the effect of the horn on the transfer impedance can estimated by

$$Z_{tf \cdot h}(s) = 1 + \frac{1}{m_{tf}} \frac{s}{\left(s - \lambda_{rm}\right)\left(s - \lambda_{rm}^{*}\right)} \qquad (5)$$

where the terms in (4) are as follows:

λ_{rm}	eigenvalue of SDOF system modelling the radiation impedance
m_{tf}	effective mass of the SDOF system modelling the transfer impedance

The accuracy of this model by comparison to the BEM data is shown in Figure 20.

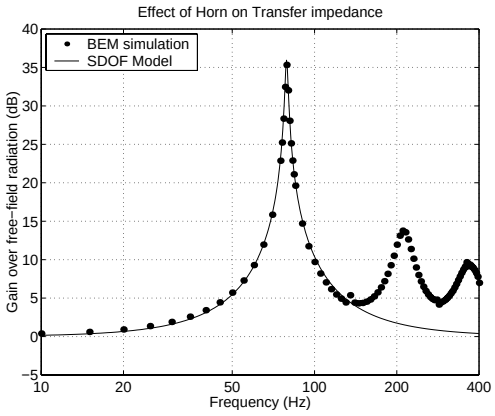

Figure 20: Effect of horn on the transfer impedance, normalised to free-field (4π) monopole radiation.

Substituting the RHS of (4) for $Z_{rm}(s)$ and the RHS of (5) in (1) results in the following expression for the far-field-pressure to voltage ratio:

$$\frac{p_{1m}(s)}{v_c(s)} = \frac{s\rho_0}{4\pi} S_d \left(1 + \frac{1}{m_{tf}} \frac{s}{\left(s-\lambda_{rm}\right)\left(s-\lambda_{rm}^*\right)} \right) \times \frac{\phi_0}{R_{eb}\left(sm_t + c_t + k_d/s + \frac{1}{m_{rm}} \frac{s}{\left(s-\lambda_{rm}\right)\left(s-\lambda_{rm}^*\right)} \right) + \phi_0^2} \quad (6)$$

where new terms in (6) are as follows:

- $p_{1m}(s)$ acoustic pressure at one (1) meter from the loudspeaker
- m_{rm} effective mass of the SDOF system modelling the radiation impedance
- R_{eb} blocked electrical resistance (DC-resistance) of the loudspeaker's voice coil
- m_t total mass of the loudspeaker diaphragm
- c_t total mechanical damping of the loudspeaker diaphragm
- k_d total stiffness, including the rear-acoustic loading, of the loudspeaker diaphragm.

Rearranging the terms in (6) into standard analogue filter form (i.e. in a ratio of polynomials in s) produces

$$\frac{p_{1m}(s)}{v_c(s)} = \frac{\rho_0}{4\pi} \frac{\phi_0 S_d}{R_{eb}} \times \frac{s^4 m_{rm} + s^3\left(c_{rm} + m_{rm}/m_{tf}\right) + s^2 k_{rm}}{\left(s^2 m_t + s c_{t\cdot e} + k_d\right)\left(s^2 m_{rm} + s c_{rm} + k_{rm}\right) + s^2} \quad (7)$$

where new terms in (7) are as follows

- $c_{t\cdot e}$ mechanical and electrical damping of the loudspeaker, i.e. $c_{t\cdot e} = c_d + \phi_0^2 / R_{eb}$
- c_{rm} effective damping of the SDOF system modelling the radiation impedance
- k_{rm} effective stiffness of the SDOF system modelling the radiation impedance

It can be shown that (7) is the product between a 2nd-order high-pass filter and a second-order band-boost filter. This can be seen in a plot of (7) shown in Figure 21, using values of the SDOF model that most closely match the BEM results. In Figure 21, the acoustic response of the loudspeaker mounted in its rear enclosure, as it would behave if the horn were absent, is plotted in green. Plotted in blue is the response using the SDOF model of (7).

It can be seen that –according to the model – the horn provides some 10dB of peak lift in the acoustic response, occurring at the resonance frequency of the SDOF system modelling the radiation impedance. This is roughly similar to the increase in output provided by a properly tuned bass reflex system. As per Figure 21, the folded horn does not, however, change the order of low-frequency roll-off; the roll-off rate remains 12dB per octave, i.e. that of a closed-box enclosure. This is in contrast to a bass reflex enclosure, which will change the roll-off rate to 24dB per octave.

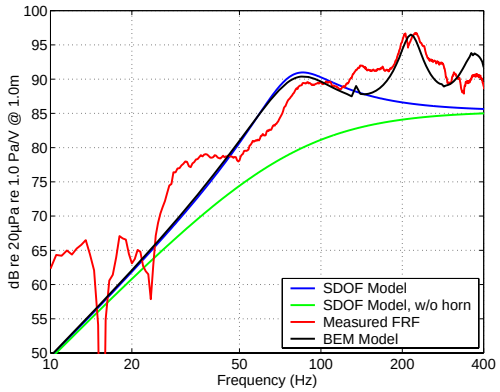

Figure 21: Pressure/voltage FRF, measured data (red), sdof model with horn (blues), without horn (green), and using the raw BEM data (black).

A disadvantage of using a folded horn is also evident in Figure 21. Using the BEM results for $Z_{rm}(s)$ and $Z_{tf}(s)$, the acoustic pressure response has peaks at 210 Hz and 360 Hz; these peaks are generally thought to result in a subjectively unfavourable sound to the loudspeaker. These peaks are the inevitable result of the peak in the transfer impedance. It should be noted that, in this study, one low-frequency horn was measured and analysed in isolation; in actual usage, this type of loudspeaker enclosure is intended to be used in stacks of four or more. Using this enclosure in stacks of multiple units is likely to reduce these peaks in the response at higher frequencies, due to the less abrupt change in the cross-sectional area of the wavefront as it leaves the individual enclosure unit. Furthermore, this type of loudspeaker is not intended to be used at frequency much higher than 200Hz, and thus these peaks would not normally be problematic.

Differences in the response between that predicted by the BEM data and the measured data (the latter of which is plotted in red in Figure 21) is assumed to be due to measurement error. The dominant source of measurement error is assumed to be a failure of the anechoic room in which this measurement was made to accurately create free-field acoustic conditions.

4. Conclusions

It has been shown that the boundary element method (BEM) can be used effectively to study the behaviour of low-frequency folded horns.

It should be noted that, even with the computational ability of computers at the turn of the millennium, solution of BEM models requires a great deal of effort from experienced engineers. To obtain useful results from BEM models requires time and patience from engineers skilled not only in the computer simulation, but also in the field of its application. Considerable time is needed to set up models and analyse their results, even if one no longer need wait days for computations to complete (as one may have some 10 years ago). Thus, for the foreseeable future, it is expected that high-order computer simulation tools such as BEM will see use mainly for 'debugging' and developing understanding of complex, unintuitive acoustical systems. The idea promoted by some in the late 1980's that BEM would become a magic wand that the engineer could wave at a complicated technical problem has, so far, proven untrue.

A single-degree-of-freedom model has been shown to be effective at modelling the first resonance of the folded horn. In the analysis of this model, it is shown that the horn provides an increase of some 10dB in the acoustic response of a loudspeaker system around the primary resonance frequency of the horn. This increase is due to the resonant nature of the horn's radiation and transfer impedance. This is in contrast to traditional horns, which provide an increase in radiation and transfer impedance over a broad range of frequencies. It is thus found that this type of horn behaves more like a bass-reflex than a traditional horn-loaded loudspeaker system.

The single-degree-of-freedom model shows that parametric study of this type of folded horn is generally possible. Such a model could be used to further study how the horn's effective flare rate could be changed to produce some other acoustic response.

5. Acknowledgements

Most research work done for this paper was done while the author was at the Institute of Sound and Vibration Research at the University of Southampton. The author would like to thank Prof. Frank J. Fahy and Dr. Keith Holland, who provided most of the inspiration and guidance for this work.

The author is grateful to Turbosound Ltd. for providing experimental equipment used in this work.

6. References

1. M. H. Knudsen, J. Grue Jensen, V. Julskjær, and P. Rubak "Determination of Loudspeaker Driver Parameters Using a System Identification Technique," *J. Audio Eng. Soc.*, **37**, pp. 700-708. (Sept. 1989)

2. Earl Geddes and David Clark, "Computer Simulations of Horn-Loaded Compression Drivers," *J. Audio Eng. Soc.*, **35**, pp. 556-566. (Jul./Aug. 1987)

3. Arthur Gordon Webster, "Acoustical Impedance, and the Theory of Horns and the Phonograph," *Proceedings of the National Academy of Sciences*, **5**, pp. 275-282. (1919)

4. C. R. Hanna and J. Slepian, "The Function and Design of Horns for Loudspeakers," *Transactions of the American Institute of Electrical Engineers,* **43**, pp. 393-404. (Feb. 1924)

5. Edward Eisner, "Complete Solutions of the "Webster" Horn Equation," *J. of the Acoust. Soc. Amer.*, **41**, pp. 1126-1145. (Apr. 1967)

6. David Bernoulli, "Physical, Mechanical, and Analytic Researches on Sound and on the Tones of Differently Constructed Organ Pipes," (in French) *Mémoires de l'Academie Scientifique*, pp. 431-485. (1764)

7. Harry F. Olson, *Acoustical Engineering*, D. Van Nostrand Company, Inc. (1957)

8. Leo L. Beranek, *Acoustics*, Acoustical Society of America, New York. (1954)

9. Keith R. Holland, Frank J. Fahy, and C. L. Morfey, "Prediction and Measurement of the One-Parameter Behaviour of Horns," *J. Audio Eng. Soc.*, **39**, pp. 315-337. (May 1991)

10. Vincent Salmon, "A New Family of Horns," *J. Acoust. Soc Amer.*, **17**, pp. 212-218. (Jan. 1946)

11 P. M. Morse and H. Feshback, *Methods of Theoretical Physics*; McGraw Hill, New York (1953).

12. Gavin R. Putland, "Every One-Parameter Acoustic Field Obeys Webter's Horn Equations," **41**, pp. 435-451. (Jun. 1993)

13. Paul W. Klipsch, "Improved Low Frequency Horn," *J. Acoust. Soc. Amer.* Vol. 14, No. 3 (Jan. 1943)

14. R. D. Ciskowski and C. A. Brebbia, *Boundary Element Methods in Acoustics*, Computational Mechanics Publications, Elsevier Aopplied Science, London. (1991)

15. T. W. Wu (ed.) *Boundary Element Acoustics: Fundamentals and Computer Codes*, WIT Press, Billerica, MA, USA. (2001)

16. A. Neville Thiele, "Loudspeakers in Vented Boxes," *Proceedings of the IRE Australia*, Vol. 22, pp.487-508 (Aug. 1961) Reprinted in *The Journal of the Audio Engineering Society*, Vol. 19, pp. 382-392. (May 1971)